Viscoelastic Relaxation of Styrene–Butadiene–Styrene Block Copolymers with Different Topological Structures

Miao Du,[1,2] Qiuming Yu,[1]* Yi Lu,[1] Qiang Zheng[1,2]

[1]*Department of Polymer Science and Engineering, Zhejiang University, Hanghzou 310027, China*
[2]*Key Laboratory of Macromolecule Synthesis and Functionalization, Ministry of Education, Hangzhou 310027, China*

Received 11 July 2008; accepted 2 September 2010
DOI 10.1002/app.33376
Published online 12 January 2011 in Wiley Online Library (wileyonlinelibrary.com).

ABSTRACT: The viscoelastic relaxation of linear styrene–butadiene–styrene triblock copolymer (*l*-SBS) and star styrene–butadiene–styrene triblock copolymer (*s*-SBS) with four arms were investigated with differential scanning calorimetry and dynamic rheological measurements. Three characteristic viscoelastic responses of *l*-SBS and *s*-SBS in the plot of the loss tangent (tan δ) and temperature at different frequencies (ω's), which corresponded to the relaxation of the polybutadiene (PB) block (peak I), the glass transition of the polystyrene (PS) phase (peak II), and the mutual diffusion between the PB blocks and PS blocks (peak III), respectively, were observed in the experimental range. Although ω was 0.1 rad/s, a noticeable peak III was gained for both *l*-SBS and *s*-SBS. The dynamic storage modulus (G') of *l*-SBS showed two distinct types of behavior, depending on the temperature. At temperature (T) $< T_2$ (where T_2 is the temperature corresponding to peak II), G' of *l*-SBS displayed a very weak ω dependency. In contrast, at $T > T_2$, G' decayed much more rapidly. However, G' of *s*-SBS displayed a very weak ω dependency at both $T < T_2$ and $T > T_2$. Only near T_2 did *s*-SBS decay with ω a little sharply. These indicated, in contrast to *l*-SBS, that *s*-SBS still exhibited more elasticity even at $T > T_2$ because of its crosslinking point between the PB blocks (the star structure). In the lower ω range, *l*-SBS exhibited a stronger peak III than *s*-SBS despite the same styrene content for *l*-SBS and *s*-SBS. The high tan δ value of peak III for *l*-SBS was considered to be related to the internal friction among the PB blocks or the whole *l*-SBS chain, not the PS blocks. © 2011 Wiley Periodicals, Inc. J Appl Polym Sci 120: 2962–2970, 2011

Key words: block copolymers; phase behavior; viscoelastic properties

INTRODUCTION

Block copolymers have great practical utility in improving the properties of homopolymer blends and of adhesives. Usually, microphase separation in block copolymers is driven by the thermodynamic incompatibility of the block constituents. Although the resulting microphase-separated morphology gives rise to useful mechanical properties, it also produces large viscosities and memory effects when it persists into the melt; this makes processing difficult. The order-to-disorder transition (ODT), or the microphase separation, in block copolymers divides the microphase-separated states and single phase. Some studies on the base of phase behavior of block copolymers experimentally determined by either rheology[1–19] or small-angle X-ray (or neutron) scattering have been reported.[20–23] Through the statistical thermodynamics method, Meier,[1] Helfand and Wasserman,[2,3] and Spontak and Zielinski[21] made extensive calculation of the chain dimensions that existed in a diblock phase-separated system and doped out the phase size. The phase diagram has also been calculated for a range of block copolymer architectures. Leibler's[13] mean-field treatment expressed the ODT for AB diblock copolymers in terms of the fraction of A units and the product χN, where χ is the Flory interaction parameter and N is the total number of monomer units in the block. The order-to-disorder transition temperatures (T_{ODT}) of several commercial thermoplastic elastomers, such as styrene–butadiene–styrene (SBS) and styrene–isoprene–styrene, are usually higher than 250°C.[15] However, their processing temperature is often lower than T_{ODT}. That is, ODT does not occur during processing for them. To control the properties, the viscoelastic relaxation in the scope of the processing temperature should be investigated. It is important to understand the rheological response for these materials in the scope of the processing temperature.

Very recently, we studied[24] the viscoelastic response of a linear styrene–butadiene–styrene copolymer (*l*-SBS) when the temperature was lower than 200°C by a combination of differential scanning

**Present address:* Hokkaido University Cooperative Pioneer Development Station, N8W5, Sapporo 060-0808, Japan.
Correspondence to: M. Du (dumiao@zju.edu.cn).
Contract grant sponsor: National Natural Science Foundation of China; contract grant number: 20304014.

TABLE I
Typical Properties of *l*-SBS and *s*-SBS

	Sample code	
	l-SBS	*s*-SBS
Topological structure	Linear	Star
Styrene/butadiene (w/w)	40/60	40/60
M_n	1.14×10^5	2.0×10^5
M_w	1.31×10^5	2.43×10^5
M_w/M_n	1.15	1.22
Molecular weight of the PS block	2.28×10^4	2.0×10^4
N_{PS}	219	192
$N_{PS}^{1/2}$	14.8	13.8
N_{PS}^2	4.8×10^4	3.7×10^4
Molecular weight of the PB block	6.84×10^4	6.0×10^4
N_{PB}	1267	1111
$N_{PB}^{1/2}$	35.6	33.3
N_{PB}^2	1.6×10^6	1.2×10^6

M_w = weight-average molecular weight. When we divided M_n of the PS block by the molecular weight of the styrene monomer (i.e., 100), we got N_{PS}. N_{PB} was obtained through the same approach.

calorimetry (DSC) and dynamic rheological measurements. The dynamic temperature sweep measurement at a constant frequency (ω) showed that three relaxation peaks appeared as the sample was heated from room temperature to 180°C; this was never reported before. As shown later, the peaks reflected the relaxation of various motion units. The properties of SBS are often determined by its topological structures, such as random, linear, star, or comb, and the corresponding viscoelastic response. To investigate the influence of the SBS topological structure on the viscoelastic response in the scope of the processing temperature, we chose two kinds of SBS block copolymers, *l*-SBS and star styrene–butadiene–styrene triblock copolymer (*s*-SBS), with the same styrene contents.

EXPERIMENTAL

Materials

l-SBS with a 40 wt % styrene content and *s*-SBS with four arms (40 wt % styrene) were supplied by Balin Petrochemical Co., Ltd. (Yueyang, Hunan Province, China). Their properties are displayed in Table I. Illustrations of the molecular structure of the two kinds of SBS are shown in Figure 1. To prevent the thermooxidation of SBS during measurement, B215, an antioxidant, was added; it was obtained from Ciba-Geigy Corp. (Basel, Switzerland). Its relative molecular weight was 647, and its melt pointing was 180–185°C.

Preparation

SBS and 1 wt % antioxidants were mixed in as Haake torque rheometer (Rheoflixer Polylab, Hennigsdorf, Germany) at 150°C for 15 min and were then compression-molded into a rectangle specimen ($35 \times 12 \times 1.5$ mm^3) or a disc specimen with a diameter of 25 mm and a thickness of 1.5 mm at 10 MPa and 150°C.

Measurements

The rheological measurements were conducted on an advanced rheometric expansion system (2ARES-9A, Rheometrics, Inc., New Castle, DE) in an oscillatory mode with a torsion rectangular geometry sample or parallel-plate geometry 25 mm in diameter. Two different types of experiment were conducted:

1. Dynamic temperature sweep tests were performed; that is, the dynamic storage modulus (G'), dynamic loss modulus (G''), and loss factor/loss tangent (tan δ) were measured under a constant ω (ω's = 0.1, 1, and 10 rad/s) with the temperatures increasing from 25 to 150°C at a rate of 2°C/min.

2. Dynamic ω sweep tests were conducted; that is, G', G'', and tan δ were measured as a functions of the angular ω, which ranged from 10^{-2} to 10^2 s^{-1}, under isothermal conditions at various temperatures, from 74 to 120°C or so. The temperature increment in the ω sweep experiment was 4°C.

The strain amplitudes in both the temperature sweep experiment and the ω sweep experiment were taken between 0.3 and 2.0% to obtain as high enough value of torque. The strains used were all in the linear viscoelastic range. To avoid the oxidation of the copolymer, a fresh sample was used for each scan. No evidence of molecular weight changes in the samples tested at or below 200°C was found by gel permeation chromatography.

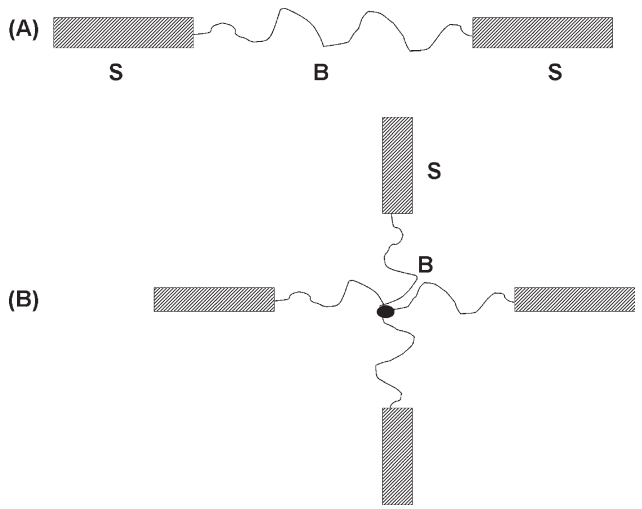

Figure 1 Illustration of the molecular structural models for (A) *l*-SBS and (B) four-armed *s*-SBS (S = styrene; B = butadiene).

The glass transition was identified by DSC. A PerkinElmer DSC-7 series was used with an internal cooling jacket capable of programmed cyclic temperature tests over a range of −150 to 400°C. Dry nitrogen gas was used for accurate measurements near the ambient temperature ranges.

The morphological study was performed on ultrathin sections (ca. 50 nm thick) obtained by low-temperature microtomy. First, SBS samples were quenched in liquid nitrogen. The ultrathin sectioning of the quenched specimens was performed by cryoultramicrotomy at −150°C; this was below the glass-transition temperature (T_g) of polybutadiene (∼−90°C). Then, the samples were stained by osmium tetroxide vapor for 24 h. A transmission electron microscope (JEM-1200EX TEM, JEOL Ltd., Tokyo, Japan), operated at 120 kV, was used to take pictures of the specimens. Therefore, in the pictures, the polystyrene (PS) phase appeared bright, and the rubbery matrix polybutadiene (PB) phase appeared dark.

RESULTS AND DISCUSSION

DSC curves

The DSC curves of *l*-SBS and *s*-SBS are shown in Figure 2. The DSC thermograms were obtained at a heating rate of 20°C/min. For *l*-SBS, two main transitions at about −90 and 65°C were observed; we considered these temperatures to be the glass transitions of the PB and PS phases, respectively. In contrast to *l*-SBS, *s*-SBS exhibited at least four transitions at about −90, −14, 74, and 100°C. As shown in Table I, *l*-SBS and *s*-SBS had almost identical number-average molecular weights (M_n's), that is, 1.14×10^5 and 2.0×10^5, respectively. The PS and PB blocks of *l*-SBS were almost the same as those of *s*-SBS, as shown in Table I. Therefore, the transitions at about −90 and 74°C for *s*-SBS should have corresponded to the glass transitions of the PB and PS phases, respectively. The other two transitions were considered to arise from the relaxation of the border layer between the PB and PS phases or a mixed PS–PB phase.[18] Compared to *l*-SBS, the relaxation of various motion units of *s*-SBS was confined because of its star structure, and as a result, it exhibited much more complex behaviors.

Morphology of l-SBS

Figure 3 presents the transmission electron microscopy photos of *l*-SBS and *s*-SBS. Morphologically speaking, *l*-SBS exhibited an alternating lamellar structure. The thickness of the PS lamellae was about 10 nm. The distance between two consecutive lamellae was about 20–25 nm. However, *s*-SBS exhibited a sea-island morphology because of its star-shape structure. The domain size of the white phase, that is, the PS phase, was also about 10 nm. That of the black phase, that is, the PB phase, was 20 nm.

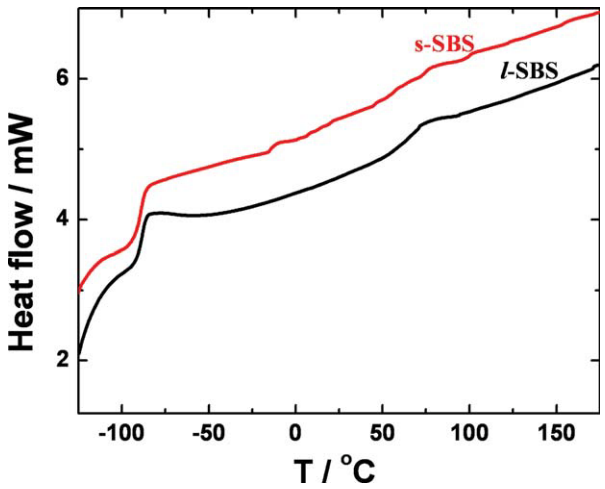

Figure 2 DSC thermograms for *l*-SBS and *s*-SBS. The curve was obtained at a heating rate of 20°C/min. The heat flows in the curves were multiplied by a factor. [Color figure can be viewed in the online issue, which is available at wileyonlinelibrary.com.]

It has been accepted that the period of microdomains of a block copolymer is on the same order as the size of a polymer chain coil (R) in the molten state,[10] that is, $R = aN^{1/2}$, in which a is the effective length of the monomer and N is the degree of polymerization. With the joint between the PS block and the PB block ignored, the polymerization degree of the PS block (N_{PS}) and the polymerization degree of the PB block (N_{PB}) for *l*-SBS and *s*-SBS were obtained cursorily, as listed in Table I, together with their square roots ($N_{PS}^{1/2}$, $N_{PB}^{1/2}$, and $N^{1/2}$). With $a = 5 \times 10^{-10}$ m for the PB block and $a = 3 \times 10^{-10}$ m for the PS block, values of $R \approx 19$ nm for PB and $2R \approx 9$ nm for PS were obtained; these values were in rough agreement with the domain size observed, as shown in Figure 3, despite the different topological structures and morphologies.

Temperature dependence of the viscoelastic response

Figure 4(A) shows the plot of tan δ versus temperature of *l*-SBS at different ω values, in which three relaxation peaks were observed. The middle peak, which was also the strongest one, was believed to be the glass transition of the PS phase, named the main transition peak (denoted as peak II in Figure 4; with its corresponding T_2). A weak peak appeared below T_2 (denoted as peak I); its corresponding temperature (T_1) increased with increasing ω. The peak at temperature (T) > T_2 was denoted as peak III, and its corresponding temperature was T_3. Both peaks I and III became more visible and moved to a lower

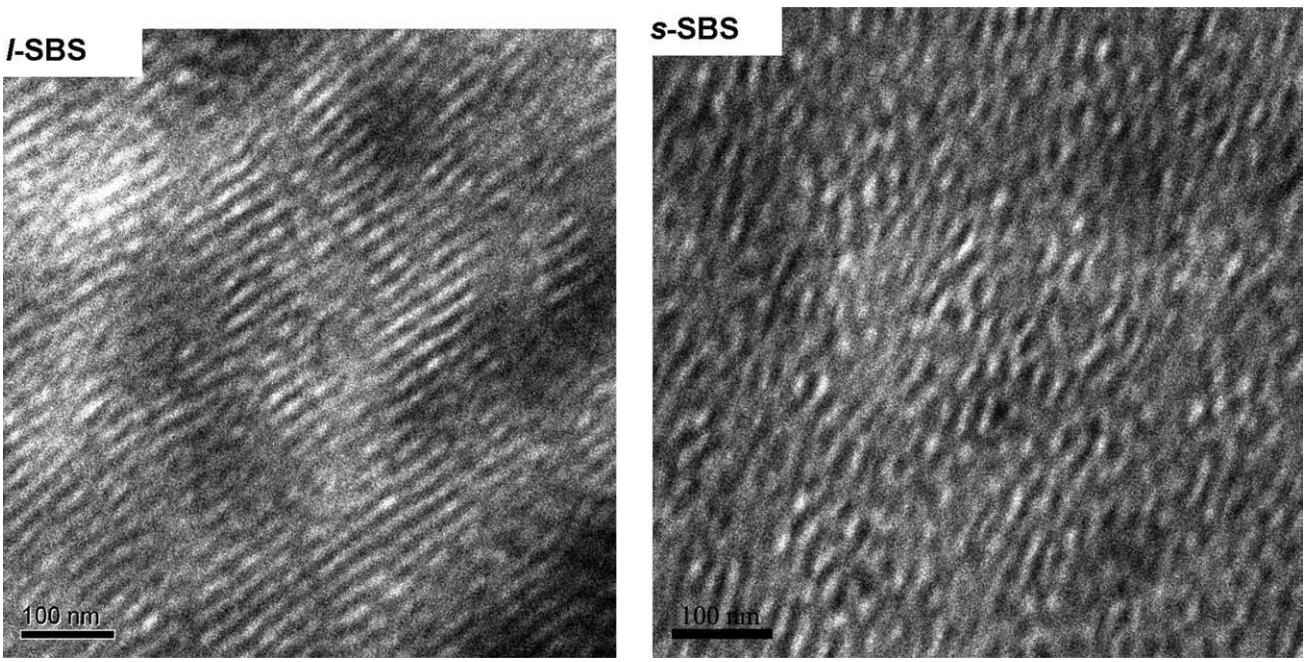

Figure 3 Transmission electron micrographs of ultrathin sections of *l*-SBS and *s*-SBS selectively stained by osmium tetroxide (the dark region represents the PB phase; the white region represents the PS phase).

temperature region as ω dropped to 0.1 rad/s. The three relaxation peaks in the plots of tan δ of *s*-SBS at different ω values are also shown in Figure 4(B), in which peaks I and III were not as obvious as those of *l*-SBS. The tan δ values of *l*-SBS and *s*-SBS as a function of the temperature at ω of 10, 1 and 0.1 rad/s are given in Figure 5, in addition to G'. In the following sections, the three peaks are discussed.

Peak I

The corresponding temperature of peak I was about 60–65°C. In this case, the PS blocks were still in a glassy state. As we know, the flow temperature of the PB homopolymer was about 0–5°C, which was much lower than T_1. Therefore, the PB blocks were in a liquid state. Thus, peak I may have reflected the characteristic relaxation of the PB block, with the two ends connecting with the PS block. Here, we recalled the behavior of the homopolymer chains with length N in a melted state. If we ignored the joint between the PS and PB blocks, the PB block could be considered a single chain. According to the tube model of Doi,[25] the reptation time (τ_t) of a PB single chain trapped inside a network can be obtained by

$$\tau_t \cong \tau_1 N^{3.3} \quad (1)$$

where τ_1 is the prefactor. τ_1 may be of order 10^{-11} s assuming that the polymer is far above T_g.

Because T_1 is far above T_g of PB, τ_1 can be considered to be on the order of 10^{-11} s.[25] For *l*-SBS, the PB chain with $N_{PB} = 1267$ led to a value of τ_t of about 0.2 s. Its reciprocal was 5 s^{-1}. For *s*-SBS, the PB chain with $N_{PB} = 1111$ led to a value of τ_t of about 0.1 s. Its reciprocal was 10 s^{-1}. ω's of 10, 1, and 0.1 rad/s gave shear rates of 2.4, 0.24, and 0.024 s^{-1}, respectively, according to the measuring mechanism of the advanced rheometric expansion system and the size of the specimens. By comparison, the shear rate of ω = 10 rad/s was close to τ_t of the PB block of *l*-SBS. *l*-SBS was, therefore, expected to have a more notable relaxation peak I than *s*-SBS during heating at an ω of 10 rad/s, although we notice that *l*-SBS had a more obvious peak I at an ω of 0.1 rad/s than *s*-SBS. In this case, the time exerted on the specimens was relatively longer, and the chemical bonds in both sides of the PB block with the PS block for *l*-SBS could not be neglected any more. For *s*-SBS, there were chemical bonds between the two PB blocks (see Fig. 1) that could be considered a crosslinking point and, therefore, hindered the relaxation of the whole PB block. Maybe the relaxation peak of the PB blocks for *s*-SBS could be observed at a much lower measuring ω.

Peak II

Both *l*-SBS and *s*-SBS exhibited strong values of peak II. Peak II was believed to be the signature of the glass transition of the PS phase. We accepted that T_g of the PS phase in *l*-SBS was lower than those of PS homopolymers (in bulk) with identical molecular weights. A prevailing opinion[19] is that T_2 of *l*-SBS depends not only on the molecular weight of the PS block (domain size) but also on the amount of SB

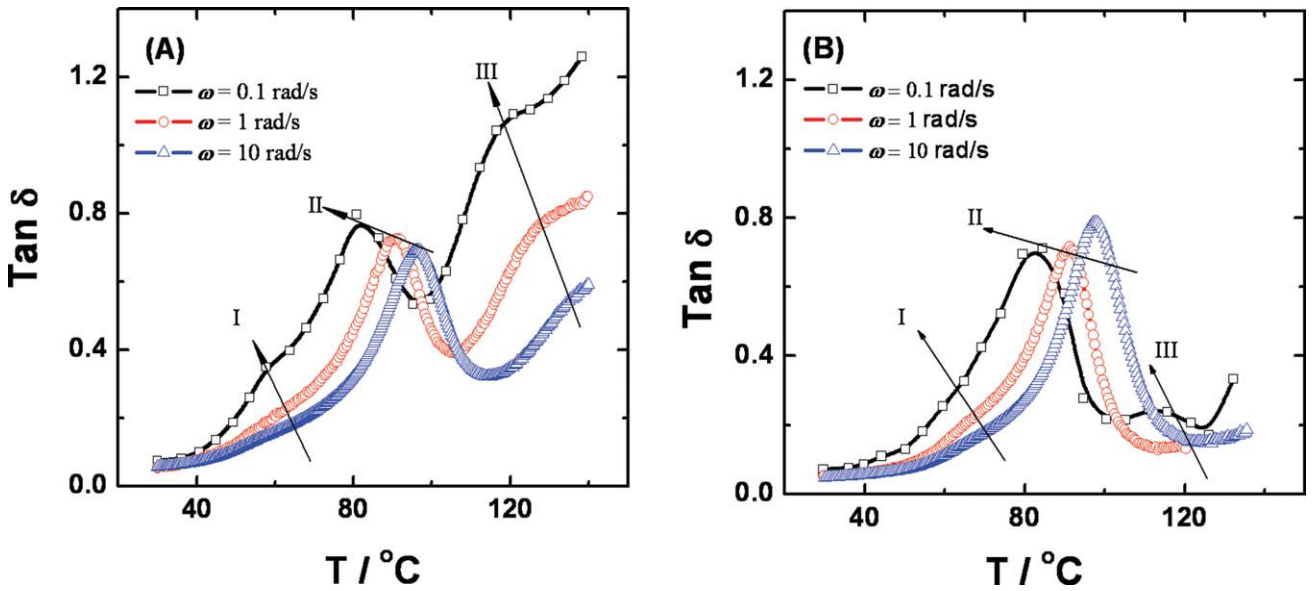

Figure 4 Temperature dependence of tan δ for (A) *l*-SBS and (B) *s*-SBS at various ω values during heating at a rate of 2°C/min. [Color figure can be viewed in the online issue, which is available at wileyonlinelibrary.com.]

segments incorporated in the PS domains. In addition, the imperfect morphology shown in Figure 3 of the *l*-SBS polymers also contributed to the lower T_2. The M_n values of the PS block of *l*-SBS and *s*-SBS, namely, 2.28×10^4 and 2.0×10^4, were lower than the critical entanglement molecular weight (M_c) of

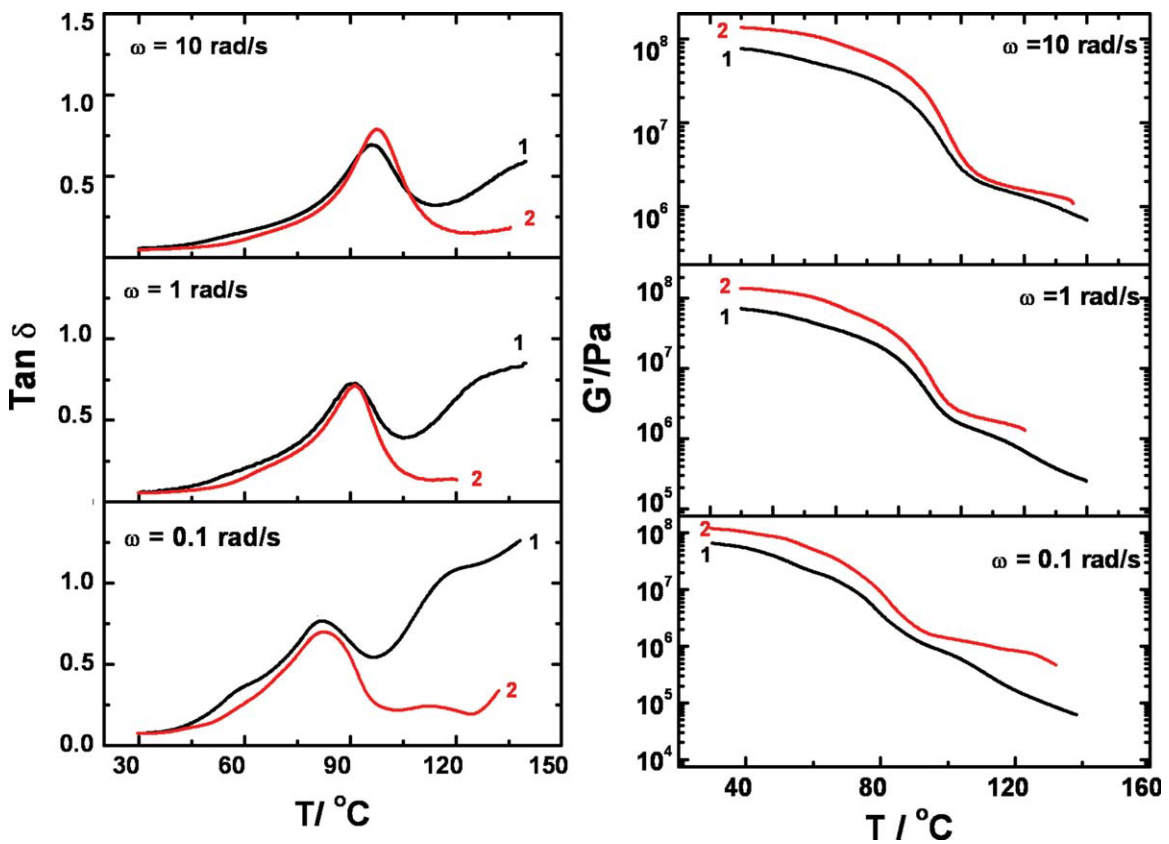

Figure 5 Tan δ and G' of (1) *l*-SBS and (2) *s*-SBS as a function of the temperature at ω values of 10, 1, and 0.1 rad/s, respectively. [Color figure can be viewed in the online issue, which is available at wileyonlinelibrary.com.]

pure PS, that is, $M_c = 3.5 \times 10^4$. With regard to the PS phase in *l*-SBS and *s*-SBS as pure PS, their corresponding T_g's should have been 95.6 and 95.0°C, respectively, according to $1/T_g = 1/373 + 0.72/M_n$;[26] this showed a tiny difference.

Peak III

Peak III became stronger at an ω of 0.1 rad/s compared to that at 1 or 10 rad/s for *l*-SBS. However, for *s*-SBS, peak III was not observed when ω was too high (e.g., 10 or 1 rad/s) during the dynamic measurements. *l*-SBS exhibited a stronger peak III than *s*-SBS and a stronger corresponding tan δ value under the same ω. Because of its linear structure, *l*-SBS easily exhibited more viscidity than elasticity, that is, a high tan δ value. However, *s*-SBS exhibited more elasticity than viscidity because of the crosslinking point between the two PB blocks. At T_3, the PS phase was in a soft state, and the motion ability of the PS blocks became stronger than that at T_2. Rubinstein and coworkers[27,28] estimated the relaxation time during melting of the lamellae for ABA-type triblock copolymers; this indicated a potential difficulty in achieving an equilibrium configuration of triblock copolymers, even significantly above the T_g's of both phases. According to Rubinstein and coworkers, the time required for A blocks to dive into the B domain is proportional to $\exp(\chi^{1/2}N_A{}^{2/3})$. However, this calculation is difficult to use if one is lacking the value of the prefactor (D_1).

If $T > T_g + 50$, τ_t of the PS block in *l*-SBS is about 5.3×10^{-4} s according to eq. (1) on the premise of ignoring the joint between the PS and PB blocks. Both Figures 4 and 5 display that T_3 was only about 20°C higher than T_g of the PS phase; thus, eq. (1) is consequently invalid. The relaxation time of the PS blocks near T_3 was accordingly expected to be much longer than 5.3×10^{-4} s. That is, in the vicinity of T_3, the PB blocks had very nice motility and behaved as viscous matter; however, the PS domains were not in a sufficiently molten state, and the motility of the PS block as a whole was still poor. Peak III was distinctly related to the mutual diffusion between the PB and PS blocks.[29,30]

The rheological signature for *l*-SBS and *s*-SBS can also be seen in the plots of G' versus T, as shown in Figure 5. G' decreased with increasing temperature. During the temperature measurement, G' of *s*-SBS was always higher than that of *l*-SBS, despite the same styrene content, because of its star structure.

ω dependence of the viscoelastic response

Figure 6 gives the ω spectra of tan δ and G' of *l*-SBS and *s*-SBS at different temperatures, respectively. G' of *l*-SBS showed two distinct types of behavior, depending on the temperature. At low temperature, G' of *l*-SBS displayed a very weak ω dependency (e.g., 80°C in A′ in Fig. 6); this indicated the signature of a crosslinking network (glass plateau) that the PS phase still maintained as a solid state and as a crosslinking point. In contrast, at high temperature, G' decayed much more rapidly (e.g., 115 and 120°C), especially at ω's below 1 rad/s. As shown by a comparison of Figures 4 and 5, the critical or transition temperature should have been T_2. However, G' of *s*-SBS displayed a much weaker ω dependency at both $T < 82$°C and $T > 102$°C, as shown in B′ of Figure 6. At 82°C $< T <$ 102°C, G' of *s*-SBS decayed with ω a little more sharply. The temperature range of 82–102°C was just the width of peak II for *s*-SBS. These indicate that in contrast to *l*-SBS, *s*-SBS still exhibited more elasticity, even at $T > T_2$.

A″ and B″ in Figure 6 display the tan δ versus ω curves at various temperatures. For *l*-SBS, the peaks appeared in the $\omega < 1$ rad/s region in the low-temperature (e.g., 85 and 90°C) region and shifted to a high ω as the temperature increased to 100°C or so but disappeared as the measured temperature further increased (e.g., 110, 115, and 120°C). Meanwhile, another peak in the low-ω and high-temperature region developed, which also shifted to a high ω with increasing temperature. In contrast, in peaks II and III of Figure 4, the peak in the low-temperature and low ω region was reckoned to correspond to the glass transition of the PS phase (i.e., peak II), and the peak in the high-temperature and low-ω region was regarded as the characteristic response of peak III. Because the dynamic rheological measurement was performed above 80°C, no peak corresponding to peak I in Figure 4 was observed. The noticeable thing was that a pronounced peak III only appeared in the region of $\omega < 1$ rad/s; this coincided with the observation of Figure 4.

To obtain the overall viscoelastic features of SBSs, the master curve of G' and tan δ over the wide ω scope for *l*-SBS and *s*-SBS derived from Figure 6 are shown in Figure 7. The reference temperature (T_r) was set as $T_r = 80$°C for *l*-SBS and $T_r = 82$°C for *s*-SBS. The G' curves measured at different temperatures superimposed well both for *l*-SBS and *s*-SBS, despite the discrepancy at the middle-ω region. Two plateaus were observed in the master curves of G'. The plateau in the high-ω region (10^0–10^2 rad/s for *l*-SBS and 10^2–10^4 rad/s for *s*-SBS) was considered to be the glass plateau of the PS phase, whereas the plateau in the middle-ω region (10^{-5}–10^{-3} rad/s for *l*-SBS and 10^{-6}–10^{-4} rad/s for *s*-SBS) was the entanglement plateau. At lower ω, an abrupt change in G' appeared, especially for *l*-SBS. Compared with G', the tan δ curves at different temperatures could not be nicely superimposed to a well-defined master curve for *l*-SBS at the lower ω region. Two distinct peaks

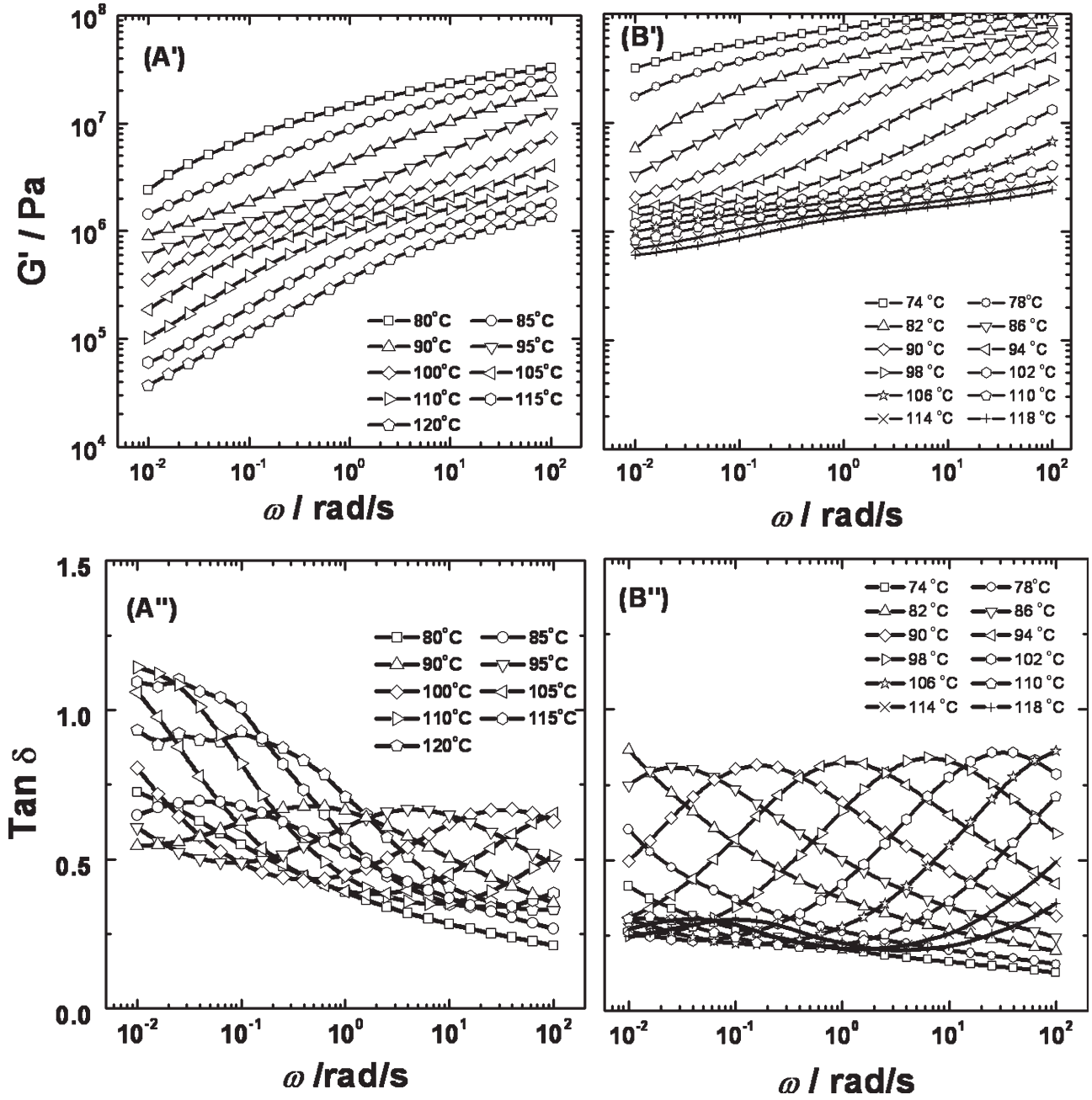

Figure 6 ω dependence of G' and tan δ for (A′, A″) *l*-SBS and (B′, B″) *s*-SBS2 at various temperatures.

corresponding to the glass transition (peak II) and peak III of Figure 4, respectively, were observed clearly; these were also denoted as peaks II and III. Peak II of *s*-SBS appeared at a relatively lower ω than that of *l*-SBS, and both exhibited a lower tan δ value than 1.0. In the low-ω range, *l*-SBS exhibited a stronger peak III than *s*-SBS; this was consistent with Figure 4. The tan δ value of peak III for *l*-SBS was higher than 1.0 and was much lower than 1.0 for *s*-SBS.

Usually, a high-quantity tan δ and wide tan δ peak are believed to dissipate a large amount of energy during the transition. The stronger peak III for *l*-SBS implied much energy dissipation. A certain amount of friction energy would have been dissipated in the form of heat around peak III because tan δ was proportional to the ratio of energy dissipated per cycle to the maximum potential energy stored during a cycle in the dynamic measurements.[31] During the dynamic measurements, the drastic internal friction of polymer chains would have brought much energy dissipation and a high quantity of tan δ. Thus, tan δ was proportional to the internal friction coefficient (f):

$$\tan \delta \propto f \tag{2}$$

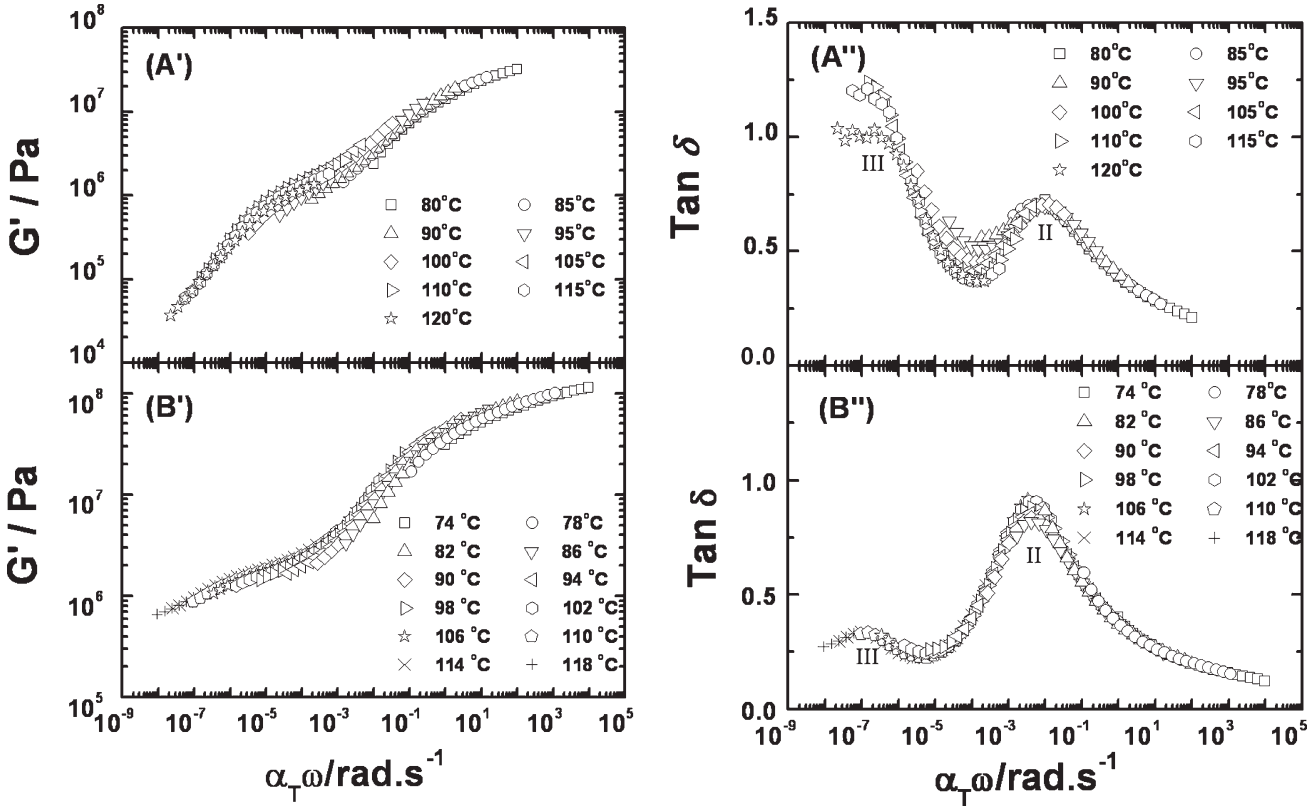

Figure 7 Master curves for G' and tan δ of (A′, A″) *l*-SBS and (B′, B″) *s*-SBS (T_r = 80°C for *l*-SBS, T_r = 82°C for *s*-SBS) (α_T = shift factor).

Three kinds of friction were involved in the *l*-SBS system around peak III: friction among the PB blocks, friction among the PS blocks, and friction between the PB and PS blocks. According to the Einstein equation of diffusion,[30] the correlation between the diffusion coefficient (D) and f was

$$D = \frac{kT}{f} \tag{3}$$

where k is the Boltzmann constant. Then, we have

$$f \propto \frac{1}{D} \tag{4}$$

Combined with eq. (2), we gain

$$\tan\delta \propto \frac{1}{D} \tag{5}$$

This equation indicates that tan δ was inversely proportional to D. From the viewpoint of the reptation of polymer chains, the PB and PS blocks were supposed as two kinds of homopolymer chains, that is, PB with a degree of polymerization N_{PB} and PS with a degree of polymerization N_{PS}. According to the scaling theory,[25] the diffusion coefficient of a reptating chain (D_{rep}) is

$$D_{rep} \cong D_1 N^{-2} \tag{6}$$

D_1 should be comparable with D in a liquid of monomers and on the order 10^{-5} to 10^{-6} cm^2/s. Then, eq. (6) could be used to estimate the diffusion coefficient of the PB block within the PB phase ($D_{rep,PB}$) and the diffusion coefficient of the PS block within the PS phase ($D_{rep,PS}$).

We dealt with the diffusion coefficient of the PB block (a long chain) giving a reptation move in the PS phase (comparative short chain), both for *l*-SBS and *s*-SBS. We considered the PB chain of N_{PB} monomers embedded in a monodisperse melt of PS, with a number N_{PS} of monomers per chain. The diffusion coefficient of the long-chain PB block ($D_{rep,N_{PB}}$) is given by

$$D_{rep,N_{PB}} = D_1 \frac{1}{N_{PB} N_{PS}^3} \tag{7}$$

With eqs. (6) and (7), the $D_{rep,PB}$ values of *l*-SBS and *s*-SBS, which were denoted as $D_{rep,PB}$(*l*-SBS) and $D_{rep,PB}$(*s*-SBS), respectively, were estimated. Likewise, $D_{rep,PS}$ of *l*-SBS and *s*-SBS were denoted as $D_{rep,PS}$(*l*-SBS) and $D_{rep,PS}$(*s*-SBS), respectively. $D_{rep,NPB}$ of the SBSs were denoted as $Ds_{rep,NPB}$(*l*-SBS) and $D_{rep,NPB}$(*s*-SBS), respectively. The N_{PB} of *s*-SBS used here was half of the N_{PB} in Table I because of the chemical bonds between the two PB blocks in

the *s*-SBS macromolecular, as shown in Figure 1. Then, we obtained

$$D_{\mathrm{rep,PB}}(l-\mathrm{SBS}) < D_{\mathrm{rep,PB}}(s-\mathrm{SBS}) \quad (8)$$

$$D_{\mathrm{rep,PS}}(l-\mathrm{SBS}) \approx D_{\mathrm{rep,PS}}(s-\mathrm{SBS}) \quad (9)$$

$$D_{\mathrm{rep},N_{PB}}(l-\mathrm{SBS}) < D_{\mathrm{rep},N_{PB}}(s-\mathrm{SBS2}) \quad (10)$$

This revealed that the low N_{PB} of *s*-SBS led to large $D_{\mathrm{rep,PB}}$(*s*-SBS) and $D_{\mathrm{rep},N\mathrm{PB}}$(*s*-SBS), and therefore, *s*-SBS exhibited a low tan δ value of peak III, despite the same styrene content for *l*-SBS and *s*-SBS. We affirmed that the high tan δ value of *l*-SBS around peak III mainly came from the internal friction among the PB blocks ($D_{\mathrm{rep,PB}}$) or the whole *l*-SBS chain ($D_{\mathrm{rep,SBS}}$), not the PS blocks ($D_{\mathrm{rep,PS}}$).

CONCLUSIONS

Three characteristic viscoelastic responses of *l*-SBS and *s*-SBS in the plot of tan δ and temperature at different ω values were observed in the experimental range, which corresponded to the relaxation of the PB block (peak I), the glass transition of the PS phase (peak II, with the corresponding temperature T_2), and the mutual diffusion between the PB and PS blocks (peak III), respectively. Only when ω was 0.1 rad/s was a noticeable peak III gained for either *l*-SBS or *s*-SBS. At $T < T_2$, G' of *l*-SBS displayed a very weak ω dependency. In contrast, at $T > T_2$, G' decayed much more rapidly for *l*-SBS. However, G' of *s*-SBS displayed a very weak ω dependency at both $T < T_2$ and $T > T_2$. Only near T_2 did *s*-SBS decay with ω a little sharply; this indicated that *s*-SBS still exhibited more elasticity, even at $T > T_2$, because of its crosslinking point between the PB blocks, namely, the star structure. In the lower ω range, *l*-SBS exhibited a stronger peak III than *s*-SBS, despite the same styrene content for *l*-SBS and *s*-SBS. We believe that the low N_{PB} of *s*-SBS led to the low tan δ value of peak III. The high tan δ value of peak III for *l*-SBS was considered to be related to the internal friction among the PB blocks or the whole *l*-SBS chain, not the PS blocks.

References

1. Meier, D. J. J Polym Sci Part C: Polym Symp 1969, 26, 81.
2. Helfand, E. Macromolecules 1975, 8, 552.
3. Helfand, E.; Wasserman, E. R. Macromolecules 1976, 9, 879.
4. Mathur, D.; Hariharan, R.; Nauman, E. B. Polymer 1999, 40, 6077.
5. Watanabe, H. J Non-Newtonian Fluid Mech 1999, 82, 315.
6. Yu-Fang, L. China Pet Chem Ind 2002, 11, 55.
7. Zhu, Y.; Gido, S. P. Macromolecules 2003, 36, 148.
8. Huy, T. A.; Adhikari, R.; Michler, G. H. Polymer 2003, 44, 1247.
9. Vinogradov, G. V.; Dreval, V. E.; Malkin, A. Y.; Yanovsky, Y. G.; Barancheeva, V. V.; Borisenkova, E. K.; Zabugina, M. P.; Plotnikova, E. P.; Sabsai, O. Y. Rheol Acta 1978, 17, 258.
10. Campos-Lopez, E.; McIntyre, D.; Fetters, L. J. Macromolecules 1973, 6, 415.
11. Adhikari, R.; Godehardt, R.; Lebek, W.; Goerlitz, S.; Michler, G. H.; Knoll, K. Macromol Symp 2004, 214, 173.
12. Hadjichristidis, N.; Pispas, S.; Floudas, G. Block Copolymers: Synthetic Strategies, Physical Properties, and Applications; Wiley: Hoboken, NJ, 2003; p 298.
13. Leiblert, L. Macromolecules 1980, 13, 1602.
14. Adams, J. L.; Graessley, W. W.; Register, R. A. Macromolecules 1994, 27, 6026.
15. Kim, J. K.; Lee, H. H.; Gu, Q.-J.; Chang, T.; Jeong, Y. H. Macromolecules 1998, 31, 4045.
16. Sebastian, J. M.; Lai, C.; Grassley, W. W.; Register, R. A. Macromolecules 2002, 35, 2707.
17. Balsara, N. P.; Dai, H. J.; Watanabe, H.; Sato, T.; Osaki, K. Macromolecules 1996, 29, 3507.
18. Masson, J.-F.; Bundalo-Perc, S.; Delgado, A. J Polym Sci Part B: Polym Phys 2005, 43, 276.
19. Mohammady, S. Z.; Mansour, A. A.; Knoll, K.; Stoll, B. Polymer 2002, 43, 2467.
20. Sakamoto, N.; Hashimoto, T.; Han, C. D.; Kim, D.; Vaidya, N. Y. Macromolecules 1997, 30, 1621.
21. Spontak, R. J.; Zielinski, J. M. Macromolecules 1993, 26, 396.
22. Du, M.; Yu, Q. M.; Wang, W. J.; Zheng, Q. Chem J Chin Univ 2006, 27, 753.
23. Floudas, G.; Hadjichristidis, N.; Stamm, M.; Likhtman, A. E.; Semenov, A. N. J Chem Phys 1997, 106, 3318.
24. Du, M.; Lu, Y.; Yu, Q. M.; Zheng, Q. Acta Polym Sinica 2008, 6, 555.
25. de Gennes, P.-G. Scaling Concepts in Polymer Physics [M]; Cornell University Press: Ithaca, NY, 1996.
26. Allen, V. R.; Fox, T. G. J Chem Phys 1964, 41, 337.
27. Rubinstein, M.; Obukhov, S. P. Macromolecules 1993, 26, 1740.
28. Witten, T. A.; Leibler, L.; Pincus, P. A. Macromolecules 1990, 23, 824.
29. Edward, V. G.; Roger, S. P. Polym Eng Sci 1977, 17, 535.
30. Sun, S. F. Physical Chemistry of Macromolecules: Basic Principles and Issues, 2nd ed.; Wiley: Hoboken, NJ, 2004; p 229.
31. Sperling, L. H. Introduction to Physical Polymer Science, 4th ed.; Wiley: Hoboken, NJ, 2005.